Thermal Unfolding and Aggregation of Human Complement Protein C9: A Differential Scanning Calorimetry Study†

Karl Lohner‡ and Alfred F. Esser*

Laboratory for Structural Biology, Department of Comparative and Experimental Pathology, University of Florida, Gainesville, Florida 32610

Received October 3, 1990; Revised Manuscript Received April 10, 1991

ABSTRACT: The thermotropic behavior of purified human complement protein C9 was investigated by high-sensitivity differential scanning calorimetry. When dissolved in physiological buffers (pH 7.2, 150 mM NaCl), C9 underwent three endothermic transitions with transition temperatures (T_m) centered at about 32, 48, and 53 °C, respectively, and one exothermic transition above 64 °C that correlated with protein aggregation. The associated calorimetric enthalpies of the three endothermic transitions were about 45, 60, and 161 kcal/mol with cooperative ratios ($\Delta H_{cal}/\Delta H_{vH}$) close to unity. The total calorimetric enthalphy for the unfolding process was in the range of 260–280 kcal/mol under all conditions. The exothermic aggregation temperature was strongly pH dependent, changing from 60 °C at pH 6.6 to 81.4 °C at pH 8.0, whereas none of the three endothermic transitions was significantly affected by pH changes. They were, however, sensitive to addition of calcium ions; most affected was T_{m1} which shifted from 32 to 35.8 °C in the presence of 3 mM calcium, i.e., the normal blood concentration. Kosmotropic ions stabilized the protein by shifting the endothermic transitions to slightly higher temperatures whereas inclusion of chaotropic ions (such as choline), removal of bound calcium by addition of EDTA, or proteolysis with thrombin lowered the transition temperatures. Previous studies had indicated the formation of at least three different forms of C9 during membrane insertion or during heat polymerization, and it is suggested that the three endothermic transitions reflect the formation of such C9 conformers. Choline, which is present at high concentrations on the surface of biological membranes, and calcium ions have the ability to shift the transition temperatures of the first two transitions to be either close to or below body temperature. Thus, it is very likely that C9 is present in vivo in a partially unfolded state when bound to a membrane surface, and we propose that this facilitates membrane insertion and refolding of the protein into an amphiphilic conformation.

Human complement protein C9 is a serum glycoprotein of 66-kDa mass (DiScipio et al., 1984). During assembly of the membrane attack complex (MAC[1] or C5b-9) of complement, the hydrophilic serum protein C9 is converted into an integral membrane protein (Esser, 1982). This refolding process is catalyzed in vivo by the membrane-bound C5b-8 precursor complex since native C9 has no affinity for biological membranes. The fully formed MAC can be imaged after negative staining or freeze-etching in the electron microscope and appears as a circular structure with an outer diameter of ≈20 nm (Tranum-Jensen et al., 1978; Tschopp, 1984a; McCloskey et al., 1989). Incubation of C9 in vitro with metal ions or trypsin leads to aggregation and formation of poly(C9) containing 12–18 C9 protomers which shows a circular structure very similar to that of the MAC (Tschopp et al., 1984; Tschopp, 1984b; Dankert et al., 1985). The structural similarities between MAC and poly(C9) have led to the proposal (Podack & Tschopp, 1982) that poly(C9) is responsible for the doughnutlike appearance of membrane-bound C5b-9 when imaged by EM. Furthermore, it was thought that both processes, completion of the MAC from C5b-8 and C9 and formation of poly(C9), proceed via similar structural C9 intermediates. Direct experimental evidence for this hypothesis was provided recently by Laine and Esser (1989), who were able to demonstrate that C9 sequence-specific antipeptide antibodies recognized refolding C9 conformers formed during C9 aggregation and during MAC formation on erythrocyte membranes. Earlier experiments by Boyle et al. (1979) had clearly demonstrated that at least two C9 conformers could be distinguished that differed from the native and the final membrane-associated conformer. The portion of the molecule embedded in the hydrophobic part of a target membrane was shown to be the C-terminal C9b fragment since it could be labeled with membrane-restricted photolabels (Ishida et al., 1982). Using information derived from sequence homologies among different proteins, susceptibility to proteases, and predictive algorithms for secondary structure elements in proteins, Stanley (1988) has proposed a five-domain model for human C9. Taken together, the reported results indicated that C9 may be a multidomain protein that unfolds and refolds during insertion into target membranes. DiScipio and Hugli (1985), using low-resolution negative-staining and immunotransmission electron microscopy (EM), challenged this view and asserted that C9 is a globular protein containing a *single* structural and functional domain. This view was somewhat modified in a later publication (DiScipio et al., 1988) by allowing for the presence of segments or modules which could be involved in binding or recognition processes within an independently folded protein domain. The cysteine-rich domains present in C9 that are also found in thrombospondin, the LDL

† This work was supported by research grants from the National Institutes of Health (R01 AI-19478) and the National Science Foundation (DBM-8516969), and by a Max Kade Foundation Fellowship to K.L.

‡ Permanent address: Institut für Röntgenfeinstrukturforschung, Österreichische Akademie der Wissenschaften, Graz, Austria.

[1] Abbreviations: DSC, differential scanning calorimetry; EM, electron microscopy; MAC, membrane attack complex; Mops, 3-(*N*-morpholino)propanesulfonate.

0006-2960/91/0430-6620$02.50/0

receptor, and the epidermal growth factor precursor were thought to correspond to such modules.

In our earlier reports, we assumed that C9 would contain separately folded domains (Ishida et al., 1982; Thielens et al., 1988; Laine & Esser, 1989), and for this reason, we wanted to obtain independent evidence for the absence or presence of such domains in C9. Differential scanning calorimetry (DSC) has played a major role in defining protein domains and for acquiring thermodynamic data on the stability of proteins and domains in general (Krishinan & Brandts, 1978; Biltonen & Freire, 1978; Privalov, 1982,; Sturtevant, 1987). Our DSC results indicate that human C9 is probably not a single domain protein and that it undergoes several transitions that may be relevant for its ability to insert into target membranes.

Materials and Methods

Proteins. Human C9 was isolated either from outdated plasma or from Cohn fraction III paste as described by Esser and Sodetz (1988). SDS–PAGE analysis of Coomassie Blue stained protein or autoradiography of radioiodinated protein indicated that the isolated protein was better than 99% pure and no proteolytic fragments could be detected. Calcium-free C9 (apo-C9) was prepared as described previously (Thielens et al., 1988) or simply produced by addition of 1 mM EDTA to the same buffer. Nicked C9 ($C9^n$) was prepared by proteolysis with α-thrombin (Dankert et al., 1985). All samples were dialyzed overnight at 4 °C into the indicated buffer, and the final dialysis buffer was used in reference measurements to provide base-line thermograms. The pH of all buffers was adjusted at room temperature. Before the calorimetric measurements, the protein solutions were routinely centrifuged in a Beckman Airfuge to remove any aggregates that may have formed during dialysis or storage. The final C9 concentration of C9, usually about 1 mg/mL, was determined spectrophotometrically by using an extinction coefficient of 9.6 mg/(mL·cm) at 280 nm (Esser & Sodetz, 1988).

Differential Scanning Calorimetry. A Microcal MC-2D instrument (MicroCal Inc., Amherst, MA) was used for calorimetric measurements at a heating rate of 60 °C/h unless otherwise indicated. The cells were pressurized with N_2 to 1.5 atm to prevent bubbling on heating, and the instrument was thermally equilibrated at 4 °C for about 1 h before the scan was started. The calorimeter was interfaced to an IBM-AT computer using a 12-bit analog/digital conversion board (Data Translation DT-2801) for automatic data collection. The DA-1 software package provided by the manufacturer was used for data acquisition and analysis. Briefly, after substraction of the stored buffer base line, the raw data (millicalories per minute) were normalized to excess heat capacity curves (kilocalories per degrees kelvin per mole) by dividing each data point by the scan rate and by the number of moles of C9 in the calorimeter cell and then digitally filtered to remove short-term noise without distortion of the peak shape. These thermograms were then used for further simulation analyses. The software provides four different subroutines to simulate the experimental data: (1) assumes all transitions are independent two-state transitions with $\Delta H_{vH} = \Delta H_{cal}$; (2) assumes independent non-two-state transitions, with H_{vH} not being equal to H_{cal}; (3) assumes sequential two-state transitions as discussed by Freire and Biltonen (1978); (4) assumes an independent two-state transition with a ΔC_p.

Results

Initial DSC experiments were performed with human C9 (1 mg/mL) in Mops-buffered physiological saline (10 mM Mops/150 mM NaCl, pH 7.2) at a scan rate of 60 °C/h.

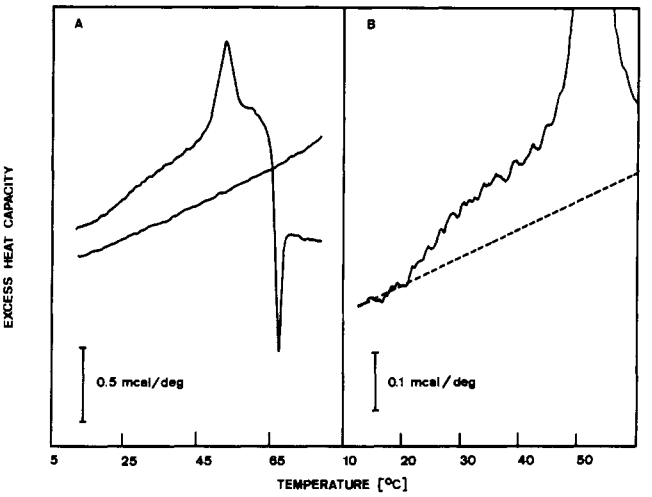

FIGURE 1: DSC thermogram of human complement protein C9. Panel A: Excess heat capacity (millicalories per degree centrigrade) curves were recorded for C9 (1 mg/mL) in standard buffer (10 mM Mops, 0.15 mM NaCl, pH 7.2) and for buffer alone at a scan rate of 60 °C/h. Panel B: Excess heat capacity curve of C9 after subtraction of the buffer heat capacity curve and displayed at 5-fold higher sensitivity to emphasize the broad transition between 25 and 45 °C. The dashed line is an extrapolation of the low-temperature base line and was used to estimate ΔC_p values.

Figure 1A shows that the protein undergoes two major thermal transitions, one endothermic centered at 53 °C and one exothermic at 68 °C. Subtracting the buffer heat capacity curve from the C9 curve verified the presence of an additional broad transition between 25 and 45 °C (Figure 1B). Such a shoulder was never observed in any buffer base line, providing confidence that it is real and not a base-line fluctuation. The base-line noise level was <8 μcal/deg while the heat capacity value at the shoulder peak at about 33 °C was 85 μcal/deg above the base line. Inspection of the sample after completion of the heating curve indicated visible protein precipitation; thus, it is likely that the observed exothermic transition resulted from protein aggregation. To check for the reversibility of heat-induced C9 unfolding, a sample was heated to 60 °C, then cooled rapidly to room temperature, and thermally reequilibrated. Rescanning of this sample revealed the absence of all endothermic transitions, and only the exothermic aggregation process occurred (data not shown). These results indicate that thermal unfolding of human C9 is an irreversible process.

Although the major endo- and exothermic transitions are separated by about 15 °C, we could not rule out that both processes, unfolding and aggregation of C9, respectively, were overlapping under our experimental conditions. Therefore, conditions were sought that might result in a better separation of these transitions. Increasing the solution pH from 6.6 to 8.0 resulted in a concomitant shift of the exothermic transition to significantly higher temperatures, whereas the temperature of the endothermic transition was only slightly affected (Figure 2A). At lower pH values, an accelerated protein aggregation prohibited accumulation of interpretable data because of overlapping endo- and exothermic transitions, and higher pH values could not be studied because of possible oxidation of the calorimeter cell. Since the aggregation rate is expected to be slower than the unfolding process, we obtained thermograms for C9 at pH 7.7 at scan rates of 30, 60, and 90 °C/h, the highest possible scan rate with this instrument (Figure 2B). The endothermic transition was affected only very slightly, but as expected, the aggregation occurred at higher temperatures the faster the scan rate. Assuming a

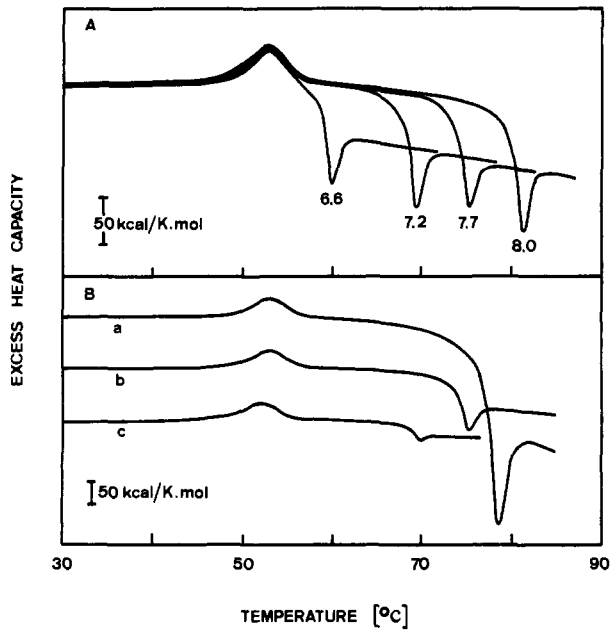

FIGURE 2: Scan rate and pH dependency of the endo- and exothermic transitions of C9. Panel A: DSC thermogram of C9 (1 mg/mL) dissolved in Mops-buffered saline at the indicated pH values. Panel B: C9 was heated in standard buffer at (a) 90, (b) 60, and (c) 30 °C/h.

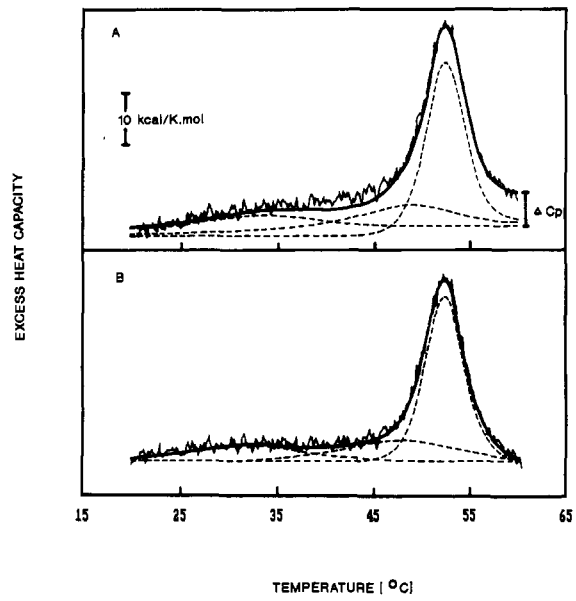

FIGURE 3: Curve simulation of C9 thermograms. The experimental raw data (before digital filtering) were fitted by assuming three independent transitions and either different ΔC_p values for the individual states using the procedure of Sturtevant (panel A) or identical ΔC_p values for the native and unfolded states as described by Freire and Biltonen (panel B).

linear dependence of the exothermic transition temperature with the scan rate, we can extrapolate to a scan rate independent aggregation temperature of about 64 °C, well separated from the thermal unfolding of C9 at 53 °C.

Thermodynamic analysis of calorimetric data traditionally required that the sample should be in thermodynamic equilibrium throughout the unfolding process. Clearly, this tenet is not fulfilled for C9 since the calorimetric transitions are irreversible. Nevertheless, recent developments pioneered by Sturtevant (Manly et al., 1985; Hu & Sturtevant, 1987; Sturtevant, 1987) and others (Sânchez-Ruiz et al., 1988) indicate that such DSC thermograms can still be analyzed. Assuming that aggregation of the protein is slow compared to denaturation, that alteration of the unfolded protein produces no heat effect in the transition range, and that unfolding can be treated as the sum of infinitesimally small equilibrium processes at temperatures lower than the irreversible denaturation, then the excess heat capacity function can be interpreted in terms of the van't Hoff equation. The fact that the major endothermic transition for C9 is scan rate independent justifies the use of this approach (Sânchez-Ruiz et al., 1988). Two different approaches were used to deconvolute the endothermic part of the thermograms into individual transitions. For the first approach, one assumes different heat capacity values for the protein in the native, intermediate, and unfolded states and sigmoidal transitions between these values. Although this procedure is strictly valid only for a simple two-state process (Takahashi & Sturtevant, 1981), it was also shown by the same group that even in more complicated systems this procedure does not introduce serious errors (Fukada et al., 1987). The difference between the ΔC_p value of the native C9 and the completely unfolded C9 can be estimated by extrapolating the pretransition base line up to a temperature just after completion of the unfolding process (Figure 3A). The ΔC_p value derived in this manner was approximately 7 kcal/(K·mol) for C9 in physiological buffers which is a typical value for globular proteins (Privalov, 1982).

Another method is based on arguments published by Biltonen and Freire (1978) and does not require knowledge of the ΔC_p value because the quantity of interest is the excess heat capacity function and its calculation is independent of the heat capacity of the unfolded state. Thus, for this deconvolution procedure, a straight base line was assumed from the beginning to the end of the transition. The calculated ΔH values obtained by using this method are affected by the uncertainty in the extrapolated slope of the base line, but the estimated errors are less than 10%, and changes in slope have little effect on T_m values (Biltonen & Freire, 1978). Figure 3 shows the fit between the experimental and the calculated data for both methods. In both cases, the best fit of the experimental curve was obtained by three *independent* two-state transitions centered at $T_{m1} \approx 33$ °C, $T_{m2} \approx 47$ °C, and $T_{m3} \approx 53$ °C. However, since success of the first method depends more strongly on accurate base-line extrapolations, *all* thermodynamic values reported here are based on simulations using the second method. Of interest is the fact that the calculated van t'Hoff enthalpy (ΔH_{vH}) is equal to the measured calorimetric enthalpy (ΔH_{cal}) for each endothermic transition reported in Table I. Equally good fitting was obtained by assuming three *sequential* transitions, and the midpoints and thermodynamic values were also similar. We have also attempted to fit the experimental curve using four two-state transitions but ended up with the same three endothermic transitions plus a fourth one whose H value approached zero as the optimization process progressed. Simulations using non-two-state transitions produced poor fits until the optimized ΔH_{vH} and ΔH_{cal} values became equal during the course of optimization, again pointing to the fact that the experimental data can best be described as the sum of three independent two-state processes. Although the first two transitions are rather broad and for this reason not very prominent in the thermogram, they provide nevertheless more than one-third of the total enthalpy change and are therefore not negligible. The measured enthalpies and transition temperatures were very repeatable provided aliquots from the same C9 preparation were used. Larger but still acceptable variations were noticed between different preparations (see Table I).

Table I: Thermotropic Properties of C9 in Different Environments

10 mM Mops buffer plus	pH	C9 lot no.	ΔH_{total} (kcal/mol)	T_{m1} (°C)	ΔH_{cal} (kcal/mol)	T_{m2} (°C)	ΔH_{cal} (kcal/mol)	T_{m3} (°C)	ΔH_{cal} (kcal/mol)	T_{exo} (°C)
0.15 M NaCl	7.2	51	260	32.1	46	48.3	57	52.5	161	67.0
0.15 M NaCl	7.2	51	260	32.6	46	48.3	60	52.5	161	67.0
0.15 M NaCl	7.2	51	260	32.5	46	48.2	61	52.4	160	67.0
0.15 M NaCl	7.2	54	275	32.0	43	47.5	62	52.6	163	69.4
0.15 M NaCl	7.4	51	268	34.9	42	48.1	66	52.6	162	68.9
0.15 M NaCl	7.7	48	248	29.6	40	45.4	43	53.0	161	75.4
0.15 M NaCl	8.0	54	280	29.6	47	45.6	55	53.0	168	81.4
0.20 M NaCl, 1.0 mM $CaCl_2$	7.4	54	270	35.4	46	49.0	59	53.4	169	66.0
0.15 M NaCl, 3.0 mM $CaCl_2$	7.2	73	270	35.8	45	48.5	61	52.7	160	58.3
0.15 M NaCl, 0.20 M Na_2SO_4	7.2	48	281	35.3	52	47.6	61	55.6	171	63.2

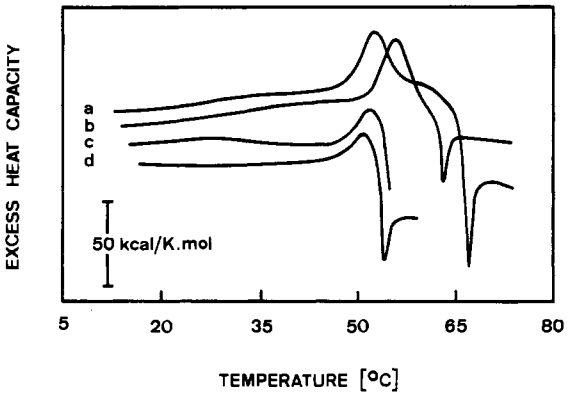

FIGURE 4: DSC thermograms of C9 in different conditions. (a) C9 dissolved in standard buffer; (b) C9 dissolved in standard buffer plus 0.2 M Na_2SO_4; (c) C9 dissolved in standard buffer plus 0.15 M choline chloride; (d) thrombin-cleaved C9 ($C9^n$) (0.7 mg/mL) dissolved in standard buffer.

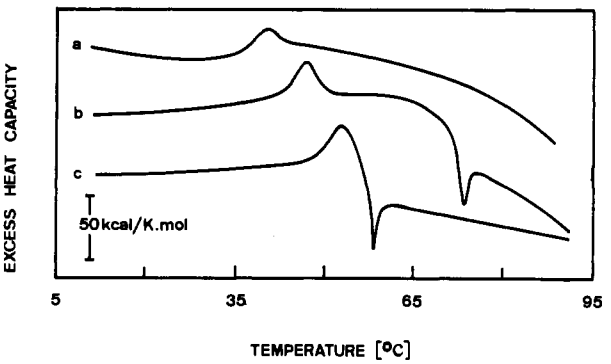

FIGURE 5: Influence of Suramin, EDTA, and calcium ions on C9 thermograms. C9 in standard buffer with additional 0.3 mM Suramin (a), or with additional 10 mM EDTA (b), or additional 3 mM $CaCl_2$ (c).

Several environmental conditions that are known to affect the activity and thermal stability of human C9 were also evaluated. For example, from previous work (Thielens et al., 1988), it is known that C9 is a calcium binding protein that is stabilized against heat denaturation by kosmotropic ions, such as sulfate, and destabilized by chaotropic ions (e.g., choline). To allow direct comparison with the previously reported data, we recorded the heat absorption of C9 in basal buffer (10 mM Mops/150 mM NaCl, pH 7.2) to which the salts of interest were added as indicated (Figure 4). DSC analysis of C9 in basal buffer plus 0.2 mM Na_2SO_4 indicated that the main endothermic transition (T_{m3}) is significantly increased but the aggregation temperature is decreased. The same trend holds true for C9 in excess Ca^{2+} (Figure 5), a condition that also resulted in the highest value recorded for T_{m1}. Table I lists the thermodynamic values for those experimental conditions in which the experimental curve could be deconvoluted with good accuracy by using the approaches discussed above.

These curve-fitting routines were not successful for thermograms of C9 under destabilizing conditions. For example, in the presence of 150 mM choline chloride, it appears that T_{m3} occurred at about 51 °C (Figure 4) and that T_{m1} and T_{m2} have shifted to below 35 °C; however, a more precise determination of the transition temperature is difficult because the aggregation process obviously started prior to the completion of the unfolding process. The same behavior was observed for nicked C9, which is known from previous work to be thermally less stable than native C9. Removal of bound calcium from C9 by EDTA resulted in markedly lower unfolding and decreased aggregation temperatures, but both remained well separated (Figure 5). Addition of Suramin lowered the main endothermic transition, and no exothermic peak below 95 °C was observed (Figure 5). In addition, it is evident that the two smaller transitions (T_{m1} and T_{m2}) are shifted to below 15 °C (Figure 5) but further experiments are required to determine the exact transition temperatures.

Discussion

Human complement protein C9 is an amphiphilic protein that is folded stably in an aqueous milieu as well as in a hydrophobic membrane environment. Key to understanding the function of this protein is to understand the refolding processes that the protein must undergo when it changes from one environment into the other. We have already initiated studies intended to identify the regions of the protein participating in this refolding process because of their recognition by C9 sequence-specific antipeptide antibodies (Laine & Esser, 1989). These studies demonstrated that conformers of C9 formed during insertion of the protein into a target membrane are also present during heat or Zn-catalyzed aggregation of C9. We have now used DSC to obtain information on such transient C9 conformers and also to identify protein domains that are involved in unfolding. The long-term goal of these DSC studies is to provide a thermodynamic basis for the existence of domains in C9 and for the interactions between domains within native C9 and membrane-bound C9. The calorimetric data presented here suggest that human C9 at physiological pH and ionic strength undergoes three thermal transitions during its unfolding process that are followed by irreversible aggregation at a temperature above 64 °C. Previous studies indicated the presence of domains in this protein, and our results would be most compatible with the assumption that the three endothermic transitions reflect the unfolding of independent domains. The fact that $\Delta H_{vH}/\Delta H_{cal}$ is close to unity suggests that each transition involves a single domain. Previous results of Boyle et al. (1979) indicated that C9 transforms into at least three different forms, called $C9^{*bound*}$,

$C9^{"inserted"}$, and $C9^{"doomed"}$, before it enters a membrane. Our own work with C9 sequence-specific antipeptide antibodies also provided evidence for at least three different C9 conformers before membrane insertion. The same or very similar conformers could also be detected during heat polymerization of C9 (Laine & Esser, 1989; Laine, 1989). We had hoped now that by separating the native molecule into two noncovalently bonded fragments ($C9^n$) through thrombin treatment we might be able to assign certain transitions to a specific portion of the molecule (see below). Unfortunately, this was not possible, and at this point in time, we do not know which transitions are associated with what part of the molecule. Future experiments with isolated tryptic or thrombic peptide fragments may yield the desired answers.

Changes in environmental conditions had significant effects on the thermal denaturation of C9. Most obvious is the effect of pH increase on the aggregation of C9; an increase from pH 6.6 to 8.0 shifted the aggregation temperature upward by about 22 °C. Studies with highly charged small molecules such as Suramin or protamine by Tschopp and Masson (1987) indicated that C9 aggregation is sensitive to charge neutralization, and these authors suggested that a cluster of negatively and positively charged amino acids is at or close to the contact sites formed during aggregation. As was predictable from these earlier data, no exothermic transition could be detected at all in the presence of Suramin (Figure 5), and the increased stability of C9 against aggregation at higher pH could result from neutralization of positive charges on the protein at higher pH. The effects resulting from removal of bound calcium ions through extraction with EDTA are also in agreement with the earlier report on the stability of the apoprotein (Thielens et al., 1988) which had clearly demonstrated a role for calcium ions in stabilization of the protein. Addition of calcium to the level present normally in human blood (3 mM) had some influence on the peak temperatures for the first two transition but had only a small effect on the main endothermic transition temperature. It is important to note that at the highest Ca^{2+} concentration, T_{m1} shifted upward to 35.8 °C (Table I), which is close to body temperature, suggesting that this transition could be of physiological significance. During purification, C9 is bound to hydroxyapatite and then eluted with a phosphate gradient (50–350 mM). Since the solubility product for calcium phosphate is low, one can expect that variable amounts of calcium will be removed from the protein during chromatography. Such uncertain amounts of calcium may explain the variability in the T_{m1} and T_{m2} values that we have observed for different C9 preparations. It may be worthwhile in the future to explore purification schemes not involving hydroxyapatite chromatography and inclusion of calcium ions into all buffers to obtain a maximally stabilized protein. The earlier reported effects of chaotropic and kosmotropic ions on C9 stability are also corroborated by the DSC measurements. Kosmotropic sulfate ions shifted *all* endothermic transitions to a higher temperature, indicating a stabilization of the total structure and not just of one domain. Yet, whereas sulfate ions stabilized the native structure, they also decreased the aggregation temperature by almost 5 °C. However, at this point, it is not clear whether this decrease is a thermodynamic or a kinetic effect since we performed these experiments at only one scan rate and one needs to know whether the extrapolated, scan rate independent aggregation temperature has changed.

The effects of choline and calcium ions on C9 unfolding are interesting since the choline group is present at high *local* concentrations on the surface of membranes in the form of lecithin. Thus, it is conceivable that C9 could undergo an *isothermal* unfolding triggered by choline and modulated by calcium ions which are also known to be tightly bound to phospholipids. The fact that T_{m1} is below or very close to the physiological temperature of 37 °C indicates that C9 is already partially unfolded at body temperature. If it can undergo further isothermal unfolding after it binds to its receptor (the C5b-8 complex) on a membrane, then this event would provide a simple mechanism for the refolding of a water-soluble protein from such a transition state into a membrane protein. For example, C9 could refold in such a way that hydrophobic surface groups become arranged in a matter compatible with the structure of an amphipathic membrane protein, whereas in solution tertiary folding would remove hydrophobic surface groups by burial in the protein core as depicted in the classical protein "oil drop" model. Other experimental evidence is also compatible with such a hypothesis. For example, the amount of secondary structure as measured by circular dichroism is nearly identical in native C9 or when bound to a membrane (Tschopp et al., 1982). In contrast, the amount of total hydrophobic surface area must be larger in the membrane-bound state of C9 because some portion of the molecule is exposed to the hydrocarbon environment of a membrane (Ishida et al., 1982). This model of C9 insertion into a membrane via a partially unfolded state can be tested in future DSC experiments. Removal of hydrophobic surfaces from the solvent during final folding of a water-soluble protein is accompanied by a large heat capacity change (Privalov, 1982; Kuwajima, 1989). Since a smaller portion of hydrophobic surface of the partially unfolded conformer needs to be buried in the membrane-bound form, one would expect significantly different heat capacity and enthalpy values for this transition pathway. Our previous studies indicated that with sequence-specific antibodies one can trap the same refolding C9 conformers during thermal unfolding and during membrane insertion (Laine & Esser, 1989; Laine, 1989), and it may be possible to use these antibodies to measure the energetics of refolding of such C9 conformers. Another possibility for generating such intermediates may be afforded by the use of denaturants in conjunction with aggregation inhibitors such as Suramin.

Limited proteolysis with thrombin cleaves C9 almost in the middle, thereby creating a nicked molecule ($C9^n$) in which two fragments, C9a and C9b, are held together noncovalently. Compared to native C9, $C9^n$ is as hemolytic and even more active in other cytotoxicity assays (Esser, 1987), but it no longer aggregates into a cylindrical polymer as does C9 and forms only stringlike aggregates (Dankert & Esser, 1985). Aggregation is, however, much facilitated with $C9^n$ as indicated by a much lower T_{m3} and a signficantly lower transition enthalpy. The higher cytotoxic effectiveness of $C9^n$ may be related to the protein's decreased stability since it should require less energy to refold into conformers competent for insertion into membranes and the rate of refolding should be significantly enhanced. Clearly knowing more about the formation of unfolding conformers of C9 in general, and especially about the energetics of the processes involved, may help in our understanding of the transformation of this water-soluble protein into an intrinsic membrane protein.

ACKNOWLEDGMENTS

We thank J. Koltai and Dr. N. Thielens for their assistance in C9 purification, Dr. J. Brandts, MicroCal, Inc., for helpful suggestions, and Drs. A. Scriabine, Miles Inc., and M. Mozen, Cutter Laboratories, Inc., for providing Suramin and Cohn fraction paste, respectively, for these studies. Some preliminary studies were carried out at the Biocalorimetry Center, The

Johns Hopkins University, and we thank Dr. E. Freire for his hospitality and for stimulating discussions.

Registry No. EDTA, 60-00-4; Ca^{2+}, 7440-70-2; SO_4^{2-}, 14808-79-8; suramin, 145-63-1; choline, 62-49-7; complement C9, 80295-59-6.

REFERENCES

Biltonen, R. L., & Freire, E. (1978) *CRC Crit. Rev. Biochem. 5*, 85–124.

Boyle, M. D. P., & Borsos, T. (1980) *Mol. Immunol. 17*, 425–432.

Dankert, J. R., & Esser, A. F. (1985) *Proc. Natl. Sci. U.S.A. 82*, 2128–2132.

Dankert, J. R., Shiver, J. W., & Esser, A. F. (1985) *Biochemistry 24*, 2754–2762.

DiScipio, R. G., & Hugli, T. E. (1985) *J. Biol. Chem. 260*, 14802–14809.

DiScipio, R. G., Gehring, M. R., Podack, E. R., Kan, C. C., Hugli, T. E., & Fey, G. H. (1984) *Proc. Natl. Acad. Sci. U.S.A. 81*, 7298–7302.

DiScipio, R. G., Chakravarti, D. N., Müller-Eberhard, H. J., & Fey, G. H. (1988) *J. Biol. Chem. 263*, 549–560.

Esser, A. F. (1982) in *Biological Membranes* (Chapman, D., Ed.) Vol. 4, pp 277–327, Academic Press, London.

Esser, A. F. (1987) *UCLA Symp. Mol. Cell. Biol. 45*, 411–422.

Esser, A. F., & Sodetz, J. M. (1988) *Methods Enzymol. 162*, 551–578.

Fukada, H., Takahashi, K., & Sturtevant, J. M. (1987) *Biochemistry 26*, 4063–4068.

Hu, C. Q., & Sturtevant, J. M. (1987) *Biochemistry 26*, 178–182.

Ishida, B., Wisnieski, B. J., Lavine, C. H., & Esser, A. F. (1982) *J. Biol. Chem. 257*, 10551–10553.

Krishinan, K. S., & Brandts, J. F. (1978) *Methods Enzymol. 49*, 3–14.

Kuwajima, K. (1989) *Proteins: Struct., Funct., Genet. 6*, 87–103.

Laine, R. O. (1989) Ph.D. Dissertation, University of Florida.

Laine, R. O., & Esser, A. F. (1989) *Nature 341*, 63–65.

Manly, S. P., Matthews, K. S., & Sturtevant, J. M. (1985) *Biochemistry 24*, 3842–3846.

McCloskey, M. A., Dankert, J. R., & Esser, A. F. (1989) *Biochemistry 28*, 534–540.

Podack, E. R., & Tschopp, J. (1982) *Proc. Natl. Acad. Sci. U.S.A. 79*, 574–578.

Privalov, P. L. (1982) *Adv. Protein Chem. 35*, 1

Sánchez-Ruiz, J. M., López-Lacomba, J. L., Cortijo, M., & Mateo, P. L. (1988) *Biochemistry 27*, 1648–1652.

Stanley, K. K. (1989) *Curr. Top. Microbiol. Immunol. 140*, 49–65.

Sturtevant, J. M. (1987) *Annu. Rev. Phys. Chem. 87*, 463–488.

Takahashi, K., & Sturtevant, J. M. (1981) *Biochemistry 20*, 6185–6190.

Thielens, N. M., Lohner, K., & Esser, A. F. (1988) *J. Biol. Chem. 263*, 6665–6670.

Tranum-Jensen, J., Bhakdi, S., Bhakdi-Lehnen, B., Bjerrum, O. J., & Speth, V. (1978) *Scand. J. Immunol. 7*, 45–46.

Tschopp, J. (1984a) *J. Biol. Chem. 259*, 10569–10573.

Tschopp, J. (1984b) *J. Biol. Chem. 259*, 7857–7863.

Tschopp, J., & Masson, D. (1987) *Mol. Immunol. 24*, 907–913.

Tschopp, J., Müller-Eberhard, H. J., & Podack, E. R. (1982) *Nature 298*, 534–538.

Tschopp, J., Engel, A., & Podack, E. R. (1984) *J. Biol. Chem. 259*, 1922–1928.